PROCEEDINGS OF SCIENCE

Study of the $K^-_{stop}\ A \rightarrow \pi^{\pm}\Sigma^{\mp}A'$ reaction on light nuclei

Paolo Camerini*
On behalf of the FINUDA Collaboration
Dip. di Fisica Univ. di Trieste, via Valerio 2 Trieste, Italy and INFN, Sez. di Trieste, via Valerio 2 Trieste, Italy
E-mail: paolo.camerini@ts.infn.it

The present paper deals with the study of the $A(K^-_{stop},\Sigma^{\mp}\pi^{\pm})A'$ reaction in p-shell nuclei, performed with the FINUDA spectrometer operating at the DAΦNE ϕ-factory (LNF-INFN, Italy). Measured spectra as well as $\pi^{\pm}\Sigma^{\mp}/K^-_{stop}$ emission rates and $\pi^-\Sigma^+/\pi^+\Sigma^-$ ratios are reported as a function of A and discussed.

8th International Conference on Nuclear Physics at Storage Rings-Stori11,
October 9-14, 2011
INFN, Laboratori Nazionali di Frascati, Italy

*Speaker.

© Copyright owned by the author(s) under the terms of the Creative Commons Attribution-NonCommercial-ShareAlike Licence.

PoS(STORI11)051

1. Introduction

The K^- and hyperon interactions with nuclei were investigated by the FINUDA collaboration via a wide program of experimental studies [1, 2, 3, 4, 5]. This was accomplished by measuring several mesonic and non-mesonic reaction channels after K^- absorption at rest on light nuclei with the FINUDA spectrometer. This allowed the study of subjects such as the A-dependence of Λ capture into nuclear bound states [1, 2] or the possibility of K^-'s forming quasi-bound states [3, 4, 5]. The present study focusses on the K^-_{stop} $A \to \pi^\pm\Sigma^\mp A'$, which is an effective tool to study the role of nuclear matter on the K^-p interaction at threshold. The K^-p interaction is strongly influenced by the presence of the $\Lambda(1405)$ below threshold and is expected to sensibly vary inside nuclear matter. The nuclear medium infact strongly affects the $\Lambda(1405)$ properties which reflects on the K^-p in-medium interaction.

The study of K^-_{stop} $p \to \pi^\pm\Sigma^\mp$ reaction on a bound proton, which is a dominant channel after K^- absorption, is therefore an effective tool to study the under-threshold behaviour.

The K^-_{stop} $A \to \pi^\pm\Sigma^\mp A'$ reaction was studied on ^6Li, ^7Li, ^9Be, ^{13}C and ^{16}O by analyzing $A(K^-_{stop}, \pi^+\pi^- n)A'$ events and reconstructing the Σ-hyperons via their decay channels $\Sigma^\pm \to n\pi^\pm$. Un unambiguous identification of the Σ together with the presence of a charged pion allows to get rid of the non mesonic Σ production as well as of the events where the Σ's have undergone to $\Sigma N \to \Lambda N$ conversion.

2. The experimental procedure

Negative kaons are the result of phi meson decays, $\phi \to K^-K^+$ (B.R.$\sim$ 50%), the ϕ's being produced almost at rest by the $e^+e^- \to \phi(1020)$ reactions at the DAΦNE collider. The kaons, emitted nearly back-to-back, traverse the beam pipe, a thin scintillator barrel [6] (TOFINO) and the inner tracking device [7](ISIM), before stopping inside the ~ 0.25 gr/cm^2 thick targets, about 20.0×5.3 cm^2 in area. The targets are arranged -as the other detectors- with cylindrical geometry around the beam axis, and are mostly solid, except for ^{13}C and ^{16}O, the first consisting of a carbon powder and the second of liquid D_2O. Besides TOFINO, placed close to the beam pipe with a diameter of 11 cm, there exists another detector made of plastic scintillator [9] (TOFONE) which consists of 72 trapezoidal slabs 2 m long and 10 cm thick organized as the staves of a barrel. While TOFINO is used for starting the time-of-flight system (tof) and for triggering purposes, TOFONE is used as the stop-counter of the FINUDA tof, which is used to determine the neutrons momentum as well as for triggering purposes.

The neutron momentum resolution was determined by measuring the monokinetic neutrons coming from the decay of stopped Σ^+ after tagging them with the π^+ emitted in opposite direction after $\Sigma^+ \to n\pi^+$ decay. The momentum distribution of such neutrons displays a peak at 187.6$\pm$0.2 MeV/c and a width of 8.4$\pm$0.2 MeV/c (σ).

In between TOFINO and TOFONE the tracking systems is placed, which consists of 2 layers of double-sided micro-strip silicon sensors [7] whose internal layer is located at about 7 cm from the trajectories of the e^+e^- colliding beams, close to the targets. The outer layer (OSIM) provides the first point of the outgoing tracks, right outside the targets, while the rest of the tracking is performed by two intermediate layers of low-mass drift chambers [8] and an outer array of straw tubes [10]

PoS(STORI11)051

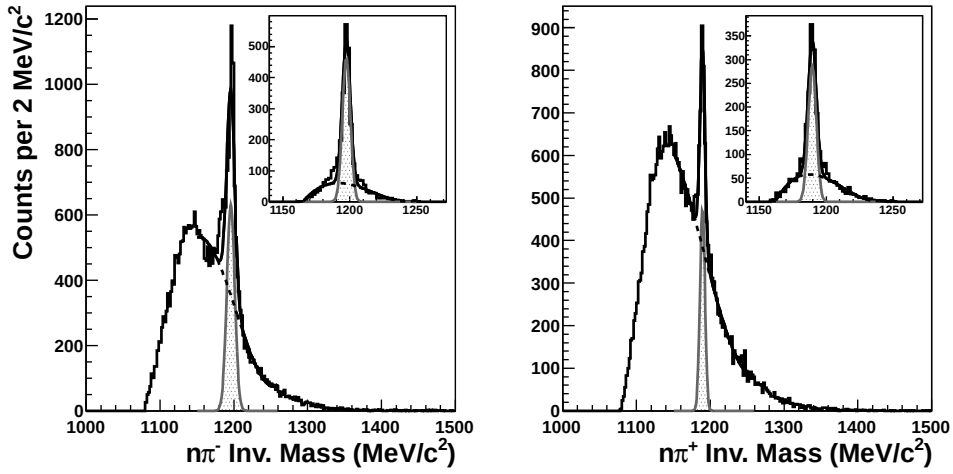

Figure 1: $n\pi^-$ and $n\pi^+$ invariant mass distributions for the ${}^6Li(K^-_{stop}, n\pi^{\mp})A'$ reaction. The hatched peaks are the Σ^- (left) and Σ^+ fitted signals. In the insets the constrained $n\pi^{\mp}$ invariant mass distributions are shown(details in the text).

which is composed of six layers, the inner being set at 111.0 cm from the colliding beams. With the FINUDA magnetic field set at 1 T, positive pions of 184.5±0.1 MeV/c are measured with a resolution corresponding to a σ of 1.72±0.06 MeV/c.

The detected $n\pi^-\pi^+$ events were filtered requiring a vertex in one of the targets between the trajectory of the initial kaon and the track of one of the two final pions. The vertex is reconstructed with an average spatial resolution of 0.7 mm, due to the relevant kaon straggling inside the target. Particle identification is performed by dE/dX techniques over the two vertex detector and the two drift chambers layers achieving an overall pion ID efficiency above 98%.

The $\Sigma^{\mp}$ were identified by means of $n\pi^-$ and $n\pi^+$ invariant mass which are shown in Fig. 1. for ${}^6Li$. The sharp peaks at 1197.0±3.4(σ) MeV/c^2 and 1189.2±3.5(σ) MeV/c^2, identify the $\Sigma^{\mp}$ signals. The background appearing in the invariant mass distributions is mainly combinatorial background due to the presence of two pions in each event, and background due to the presence of gammas which may emulate neutrons in TOFONE, and to neutrons which may scatter before being detected.

A relevant background reduction is obtained by requiring the kinematic observables of the $n\pi^{\mp}$ events to belong to the phase space volume of the $\Sigma^{\mp} \to n\pi^{\mp}$ decays as can be seen in the insets of Fig. 1: the signal (S) to background (B) ratio obtained with such a constraint is $(S/B)_{\Sigma^-}$=4.5 and $(S/B)_{\Sigma^+}$=3.6, being S the area of the hatched peaks taken at 2σ.

3. Results

The missing masses, the momentum distributions and the emission rates which will be discussed in the following, are scarcely affected by the presence of background due to the quasi-exclusive character of the reaction studied, which allowed to get rid of most of the quasi-free background reactions. Fig. 2 shows the $(K^-_{stop}, \pi^{\pm}\Sigma^{\mp})$ missing mass (M) spectra of ${}^6Li$, formed with the same data constrained to belong to the hatched peak in the inset of Fig. 1.The nominal

PoS(STORI11)051

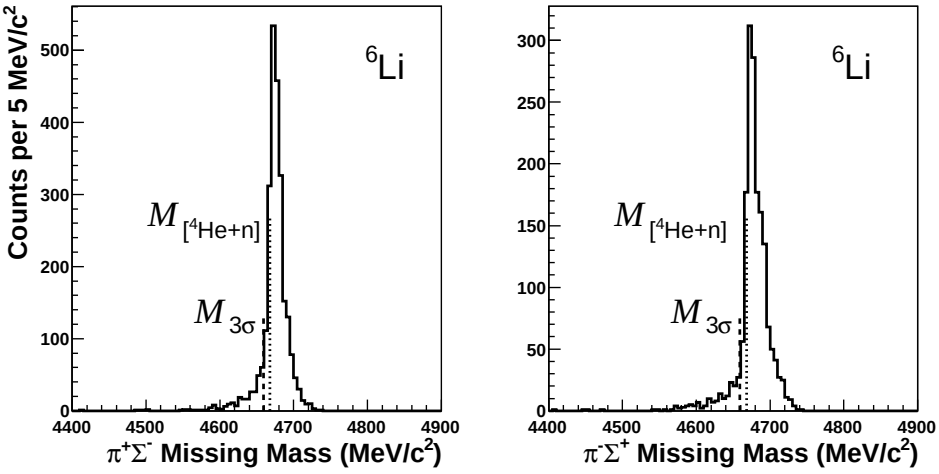

Figure 2: Missing mass distribution for the ${}^6Li(K^-_{stop}, \pi^{\pm}\Sigma^{\mp})A'$ reactions. The dash-dotted line indicates the physical threshold of the missing mass, while the dashed line indicates the lower threshold chosen for the analysis.

physical threshold ($A' = [{}^4He + n]$) of the missing mass and the one taking into account (at a 3 σ value) the σ=3.1 MeV/c^2 experimental resolution are indicated with dashed and dashed-dotted lines respectively. It is interesting to note that both distributions are peaked at about 10 MeV/c^2 above threshold with a FWHM of 22-24 MeV/c^2. This is an indication of the quasi-free nature of the reaction, with more than 96% of the energy being carried by the detected particles. This also suggests that the outgoing detected particles are scarcely distorted by final state interactions, while the value of the average missing energy could be explained by the energy loss sufferred by the $\pi^{\pm}\Sigma^{\mp}$ pairs while travelling inside the target medium or by excitation of the residual nucleus. Similar conclusion can be drawn for the other examined nuclei (figure not shown).

In Fig. 3. the measured momentum distributions of prompt pions after acceptance correction are shown for all the measured targets. Grey-filled histograms refer to negative pions, open histograms to the positive ones. The arrows indicate the phase-space limit for the $\Sigma^{\pm}$ to be unbound. The shapes of the pion distributions slightly vary with A, the main difference appearing when comparing the positive to the negative distributions, which differ mainly because of the different phase space-limits related to the Σ^+-Σ^- mass difference. Negligible distortions are expected because of the pions traversing the thin target medium. Fig. 4.shows the measured $\Sigma^{\pm}$ momentum distributions (grey-filled hystograms) for the ${}^6Li$ targets, as determined by measuring the momenta of their decay products. While the Σ^- distribution bears a rather symmetric shape, 160MeV/c wide, a narrow peak appears in the Σ^+ momentum distribution at around 0 MeV/c. The Σ^- (Σ^+) decaying in flight have an average momentum of 160 MeV/c (174 MeV/c). At such low momenta there is a relevant probability for the Σ's to loose all of their energy by collision energy loss in the target and stop. Once at rest the the Σ behaviour strongly depends on its charge: while the Σ^+ decays free, the Σ^- is captured by a target nucleus and later undergoes a Σ-Λ conversion. Since Λ-hyperons are not considered in the present analysis the Σ^- momentum distribution shows no strength at around 0 MeV/c.

In order to better undertand the measured momentum distributions, a Monte-Carlo code was

PoS(STORI11)051

developed, which employs the $K^-_{stop}A \rightarrow \pi^{\pm}\Sigma^{\mp}A'$ quasi-free reaction to generate the Σ momentum spectra and filters then the spectra through the geometry of FINUDA, which also accounts for the interaction of $\Sigma^{\mp}$ with the target media. The resulting momentum spectra before (full dots) and after (open histograms) filtering are finally compared with the measured momentum spectra showing a reasonable overall agreement.

Similar shapes as for ^6Li are found for the other target nuclei studied, which indicates a rather weak dependence on A of the reaction for p-shell nuclei, consistently with the fact that Σ-Λ conversion in not contributing to the measured spectra.

The $\pi^{\pm}\Sigma^{\mp}/K^-_{stop}$ emission rates R_A were also evaluated and are displayed as a function of A in Fig. 5. (top) together with older measurements results on ^4He [11] and ^{12}C [12]. The values are corrected for the amount of unobserved Σ^-'s as deduced from the value of at rest decay in the Σ^+'s measured momentum distributions.

In the lower part of Fig. 5 the ratio R_{+-} between $R_A(\pi^-\Sigma^+)$ and $R_A(\pi^+\Sigma^-)$ is reported for several nuclei (see figure caption for details).

While the R_A rates appear to be rather strongly dependent upon nuclear structure (see for example the change in strength when going from ^6Li to ^7Li or from ^{12}C to ^{13}C) the R_{+-} behaviour is much less dependent on A: if the K^-_{stop} $p \rightarrow \pi^{\pm}\Sigma^{\mp}$ reaction occurs inside a nucleus then $R_{+-} > 1$, ranging from 1.8 on ^4He to 1.3 on ^9Be to 1.2 on ^{16}O. A major change is seen on the contrary if the same process occurs on a free proton where the ratio is less than 1 (R_{+-}=0.42 on H [13]). Such a behaviour is probably to be related to the sub-threshold modification of the $\bar{K}N$ interaction inside nuclear matter and is therefore be an interesting testing ground for $\bar{K}N$ theoretical models.

The mean value of R_{+-} is 1.3±0.1, which is in accordance with the prediction of Ref.[14] for nuclear skin densities in the range 0.0 to 0.35 of nuclear saturation density. The observed flat behaviour of R_{+-}, consistently with the missing mass behaviour, is an indication of the fact that the K^- absorption preferentially takes place at the nuclear surface on the light nuclei examined.

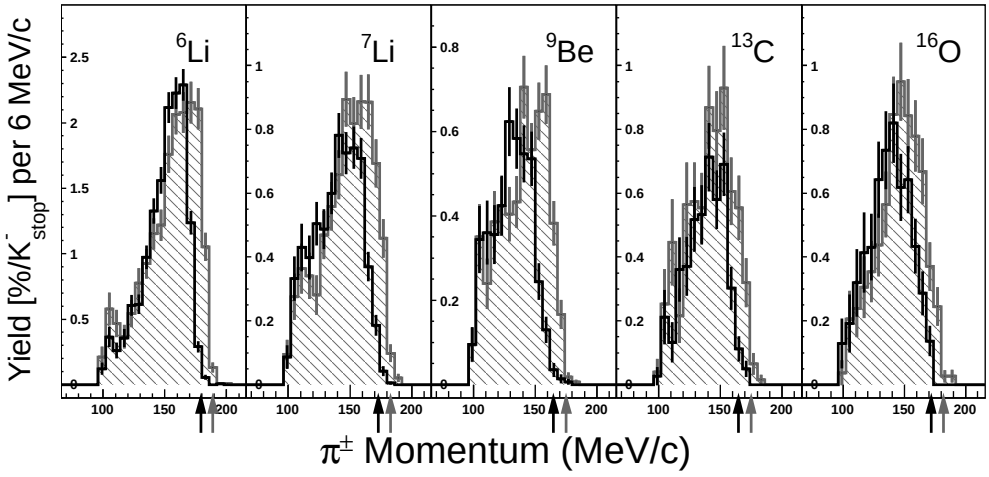

Figure 3: Measured momentum distributions of prompt pions from the $A(K^-_{stop}, \pi^{\pm}\Sigma^{\mp})A'$ reactions. The open (hatched) histograms refer to positive (negative) pions while the black (grey) arrows point to the p$[B_{\Sigma^{-(+)}} = 0]$ threshold.

PoS(STORI11)051

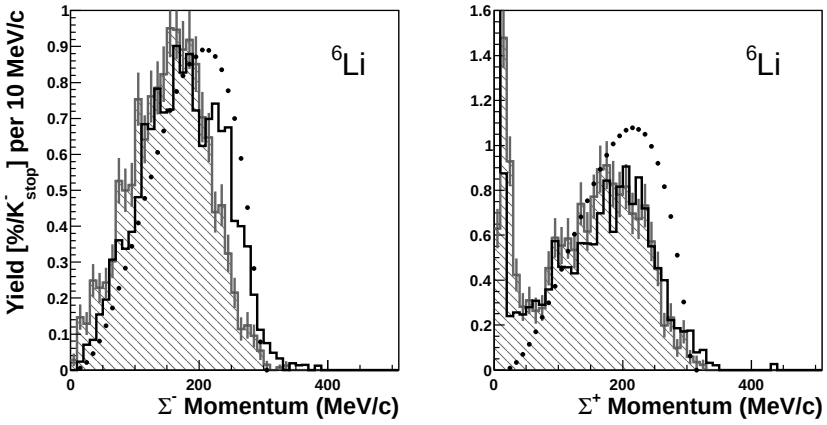

Figure 4: Momentum distributions of Σ's from the ${}^6Li(K^-_{stop},\pi^{\pm}\Sigma^{\mp})A'$ reactions. The hatched histograms are the measured distributions. The Monte-Carlo generated distributions of are depicted by full dots while with open diagrams are represented the M-C generated sigmas being reconstructed by FINUDA.

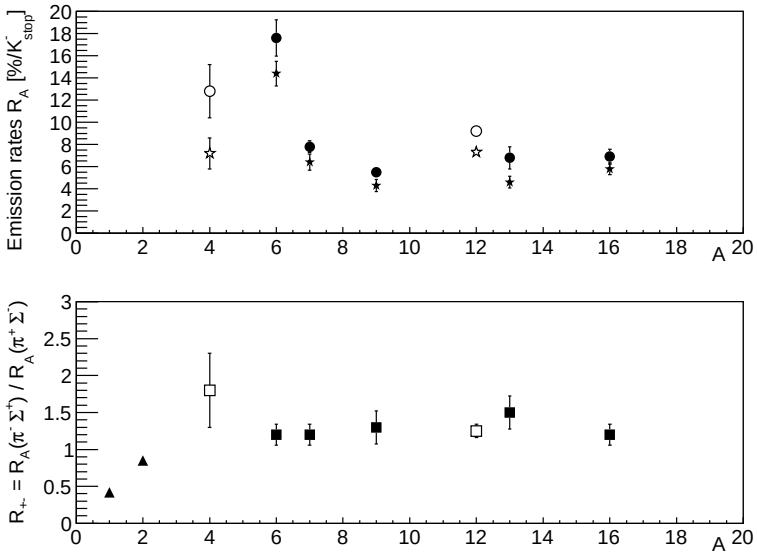

Figure 5: Top: R_A for $\pi^-\Sigma^+$ (circles) and $\pi^+\Sigma^-$ (stars) as a function of A, where R_A is given in units of $[10^{-2}/K^-_{stop}]$. Filled sysmbols are from FINUDA. The R_A values are followed by the statistical and systematic uncertainties. Σ^-_{loss} is expressed in units of [%]. The emission rates of ${}^4He$ and ${}^{12}C$ are taken from Refs. [11] and [12], respectively. Bottom: The ratio R_{+-}=$R_A(\pi^-\Sigma^+)/R_A(\pi^+\Sigma^-)$ is shown. Black squares are from FINUDA, ${}^4He$ is from ref. [11], ${}^{12}C$ from [12], H and ${}^2H$ from [13])

PoS(STORI11)051

References

[1] M. Agnello et al., Phys. Lett. **B622** (2005) 53.

[2] M. Agnello et al., Phys. Lett. **B698** (2011) 219.

[3] M. Agnello et al., Phys. Rev. Lett. **94** (2005) 212303.

[4] M. Agnello et al., Phys. Lett. **B654** (2007) 80.

[5] M. Agnello et al., Phys. Lett. **B669** (2008) 229.

[6] V. Filippini et al., *Nucl. Instr. and Methods* **A424** (1999), 343.

[7] P. Bottan et al., Nucl. Instr. and Methods **A427** (1999) 423.

[8] M. Agnello et al., Nucl. Instr. and Methods **A385** (1997) 58.

[9] A. Pantaleo et al., Nucl. Instr. and Methods **A545** (2005) 593.

[10] L. Benussi et al., Nucl. Instr. and Methods **A361** (1995) 180;
L. Benussi et al., Nucl. Instr. and Methods **A419** (1998) 648.

[11] P.A. Katz et al., Phys. Rev. **D1** (1970) 1267.

[12] C. Vander Velde-Wilquet et al., Nucl. Phys. **A241** (1975) 511.

[13] R. J. Nowak et al., Nucl. Phys. **B139** (1978) 61.

[14] S. Wycech, Nucl. Phys. **B28** (1971) 541.

PoS(STORI11)051